

Change in the Precipitation Intensity over East Asia and in Tropical Cyclone Frequency in the 228-year Simulations by a Global Atmospheric Model with 60-km Grid Size

Tosiyuki Nakaegawa and
Global Modeling Group

Meteorological Research Institute



SOUSEI Program for Risk Information
on Climate Change
気候変動リスク情報創生プログラム

Contents

The 228-year simulations with a global atmospheric model with 60-km grid size

1. Reproducibility and projections in the precipitation intensity over East Asia by Kusunoki and Mizuta (2013) in JGR
2. Decreasing trend in tropical cyclone frequency by Sugi and Yoshimura (2012) in GRL

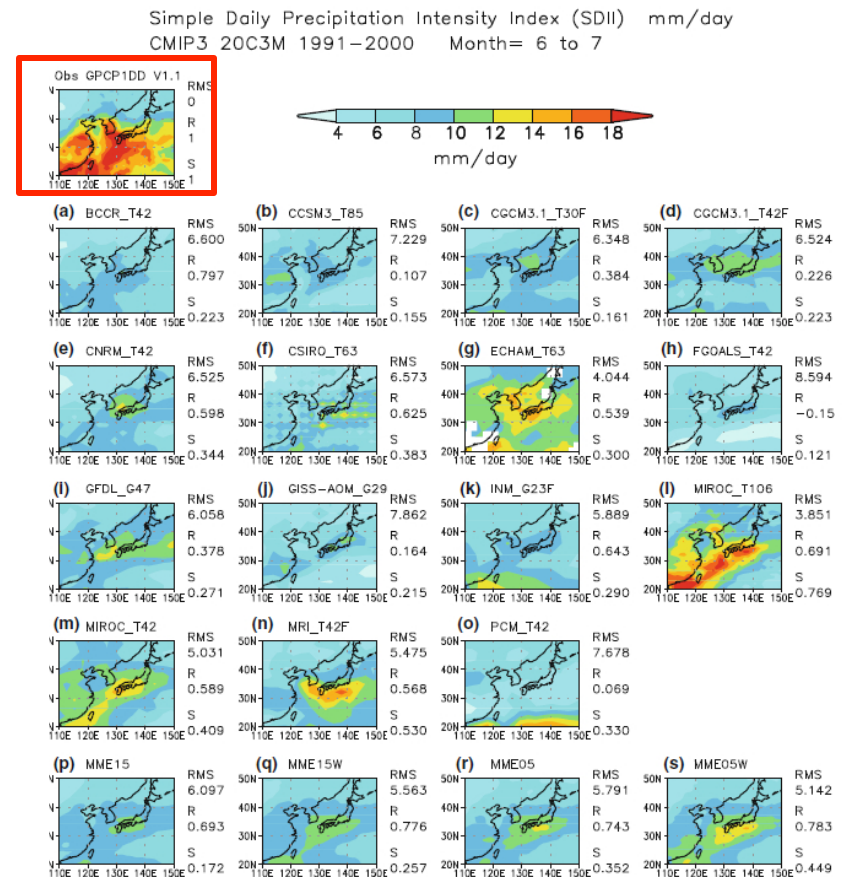


Background

for reproducibility in the precipitation intensity over East Asia

- Most climate models underestimate precipitation intensity mainly due to low horizontal resolution.
- These systematic biases reduce the reliability of future climate projections with GCMs.

How does a high horizontal resolution model capture the precipitation intensity and project future changes?



e as Fig. 1, but for Simple Daily precipitation Intensity (SDII) for June to July. Climatology is calculated only if SDII or whole years of target period at each grid point. No shading region denotes missing data. The five best models based on S of SDII are model e, f, l, m, and n

MRI-AGCM3.2H

Item	Content
Horizontal resolution	60km , TL319
Vertical resolution	64 levels 0.01 hPa top
Time step	15 minutes
Cumulus	Yoshimura (AS/Tiedke hybrid)
Cbud	Tiedtke (1993)
Radiation	JMA (2004r1)
Gravity drag	Iwasaki et al (1989)
Top condition	Rayleigh friction
Sea surface	MRI-scheme + skin SST
Land surface	SB0109
Boundary layer	Melbr-Yamada Level 2
Aerosol direct	5 species
Aerosol indirect	None

Experimental Setup

Experimental Setup

- Integration period: 1872 to 2099
- Ensemble Size: 3
- Boundary conditions : in the next slide



Boundary conditions and External Forcings

Period	1872-2000	2001-2005	2006-2099
SST and Sea ice	HadISST1		HadISST+CMIP3 Multi-model ensemble, A1B
Sea ice thickness	Observed climatology Bourke and Garrett (1987)		CMIP3 Multi-model ensemble, A1B
Greenhouse Gas	CO ₂ ,CH ₄ ,N ₂ O,CFC Observation	CO ₂ ,CH ₄ ,N ₂ O,CFC A1B	
Aerosol	MRI-ESM, 5-year average, A1B - Volcanic eruption: Oct 1986 - Present - Before 1970: 1969-1973 average - After 2097: 2092-2096 average		
Ozone O ₃	MRI-CCM CCMVal , 5-year average, A1B - Before 1960: 1959-1963 average		



Precipitation Indices

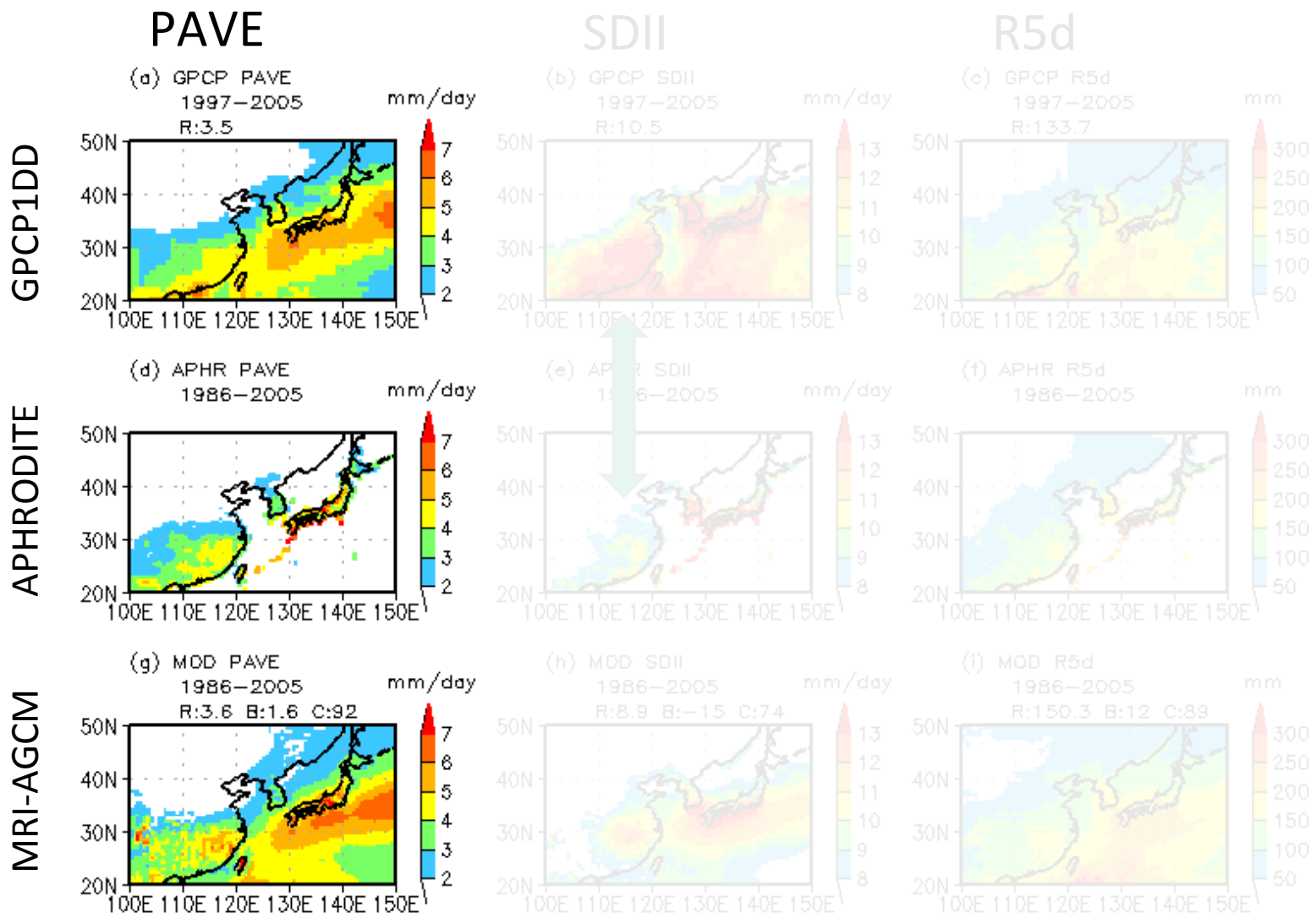
Name	Variable	Unit
PAVE	Annual precipitation	mm/ day
SDII	Simple Daily precipitation Intensity Index Total precipitation / number of rainy days rainy day : Precipitation ≥ 1 mm/day	mm/ day
R3d	Maximum 3-day precipitation total	mm
R5d	Maximum 5-day precipitation total	mm
R10d	Maximum 10-day precipitation total	mm



Observational Precipitation data

Name	Period	Horizontal Resolution	Time Resolution	Region
GPCP 1DD v1.1	1997-2008/ 12 years	1.0 deg	Daily	Global
APHRODITE	1951-2007/ 57 years	0.25 deg	Daily	Asia/ Land Only

Climatological Index Values



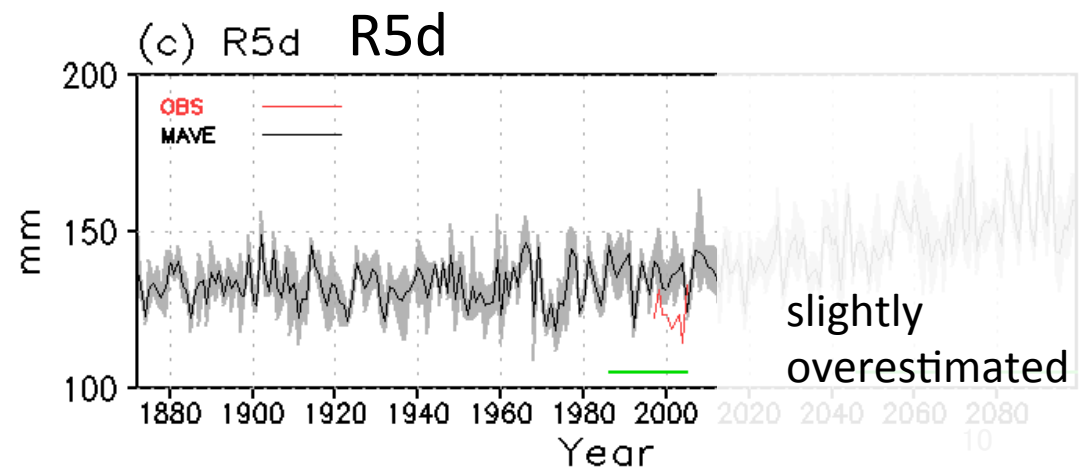
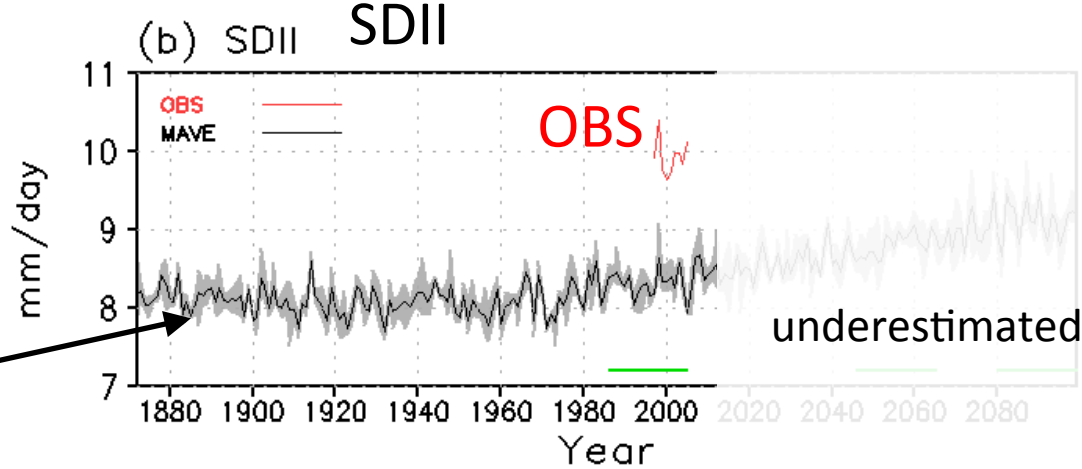
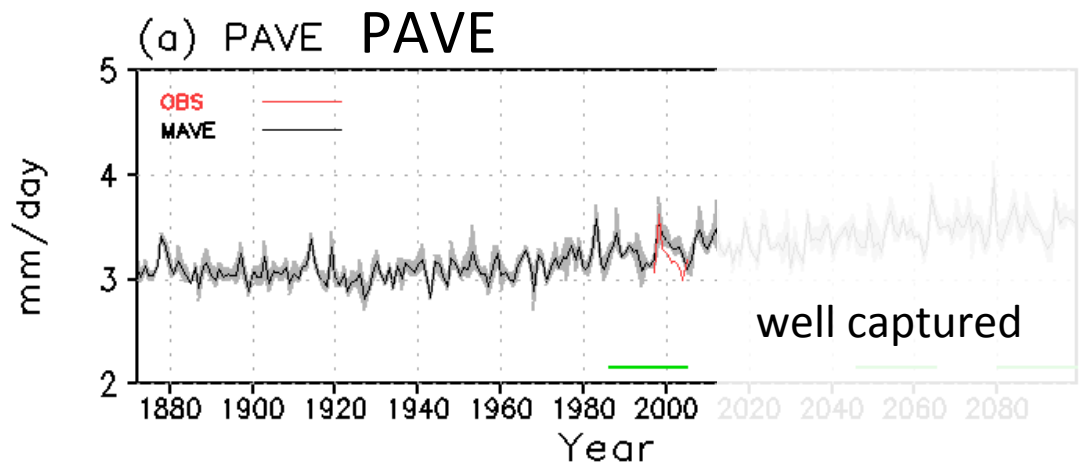
Kusunoki and Mizuta (2013, JGR)



Regional Average (100-150E, 20-50N)

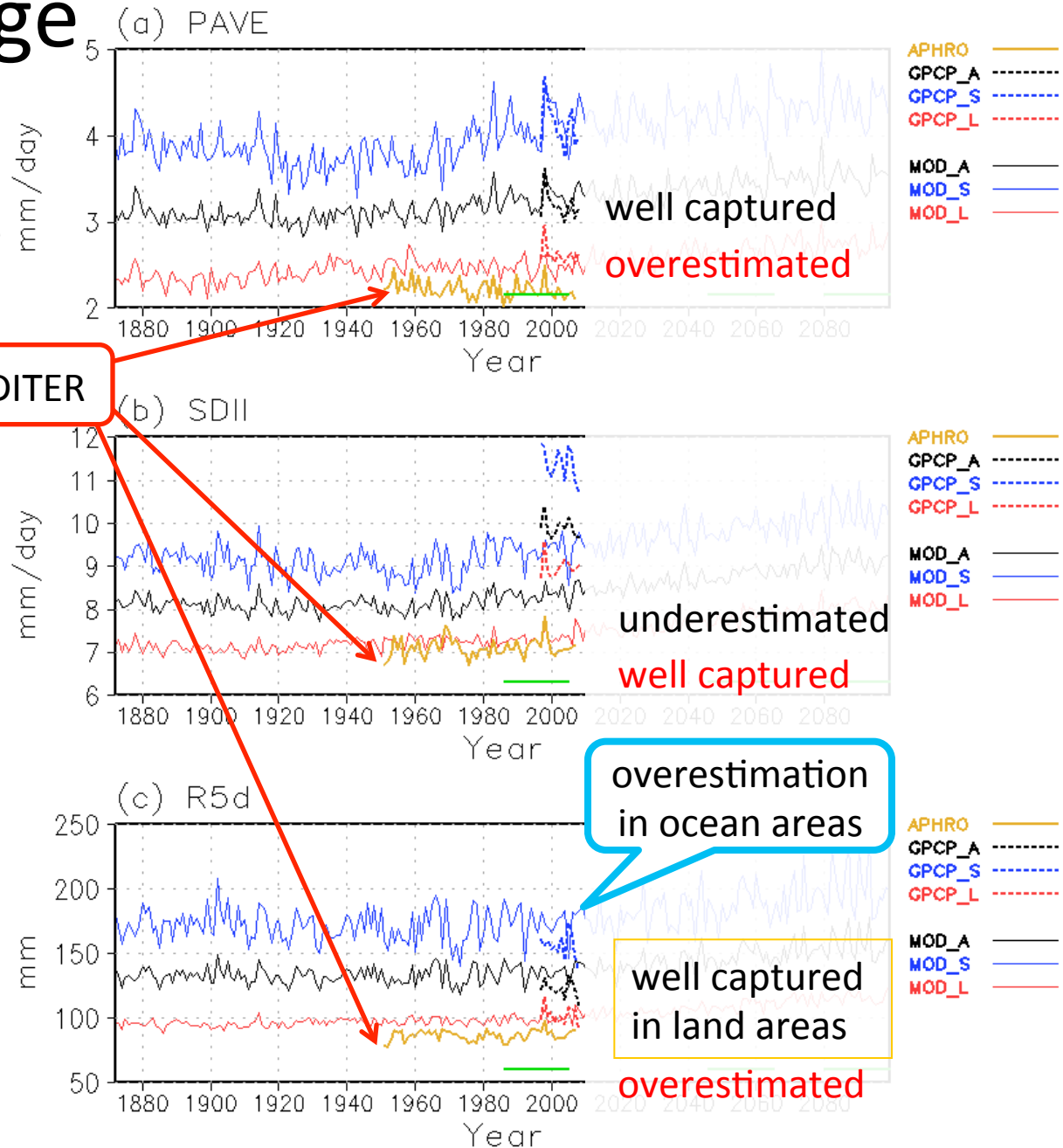
Thick black line:
Model Ensemble
Average

Gray shade:
Range of individual runs



Regional Average All/Sea/Land (100-150E, 20-50N)

APHRODITER



Changes relative to present-day climate: 1986-2005

PAVE

SDII

R5d

Change (%) Season=ann

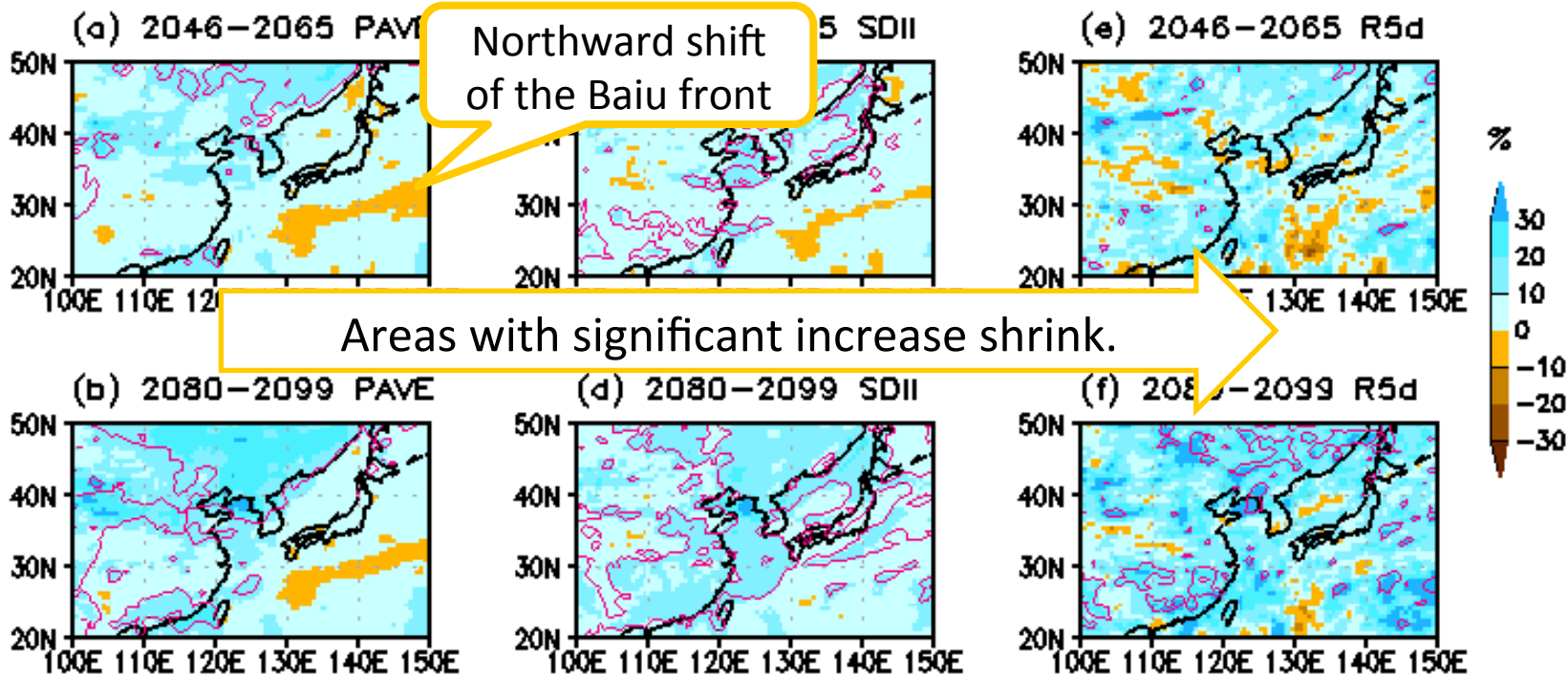
Present-day: 1986-2005, 20 years

Contour: 95% significant

2046-2065

Increase

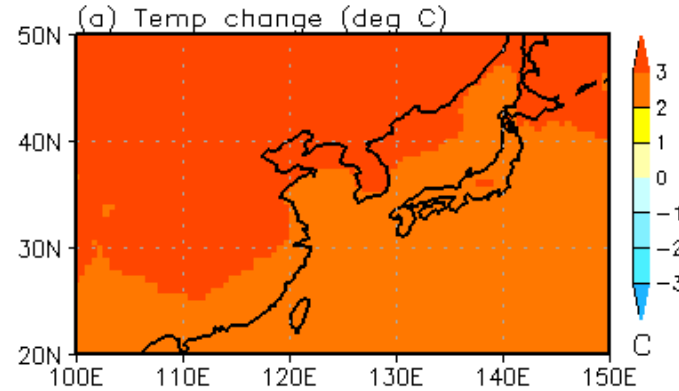
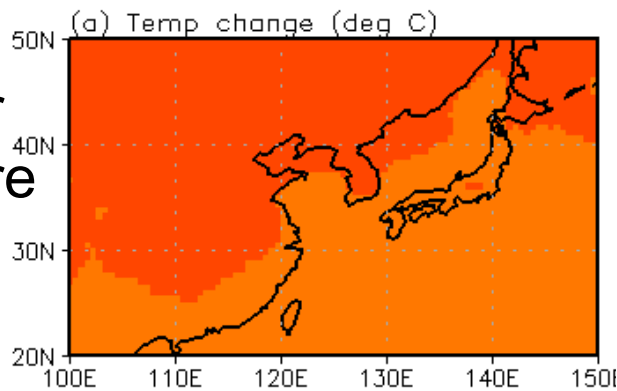
2080-2099



Ensemble average

Change per 1deg C warming

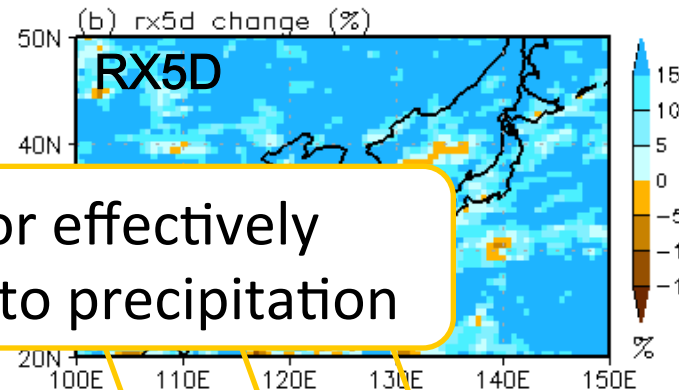
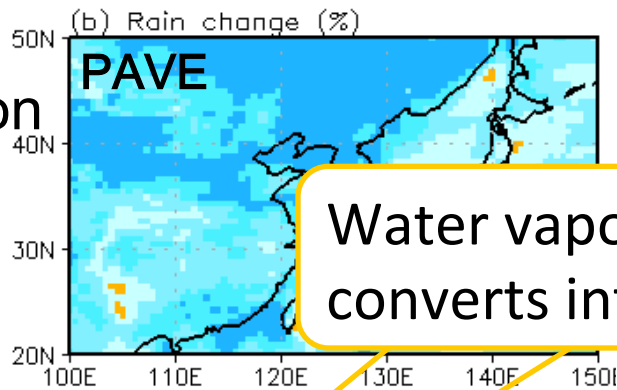
Surface air temperature change



Present: 1986-2005
Future : 2080-2099

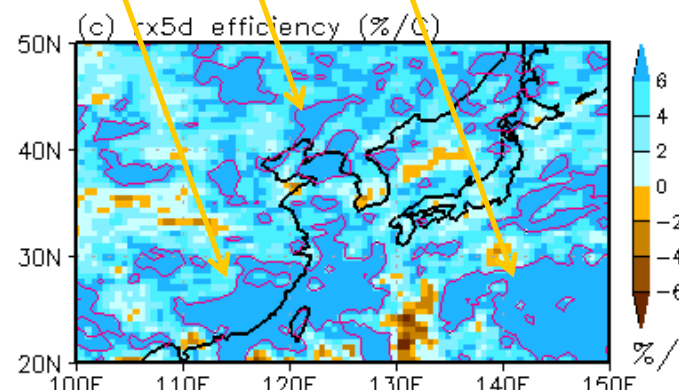
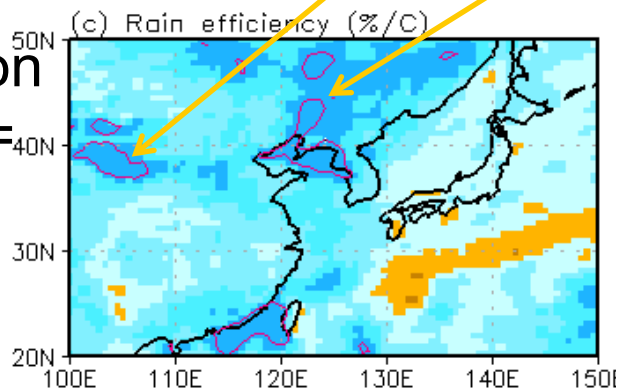
Ensemble average

Precipitation change



Water vapor effectively converts into precipitation

Precipitation efficiency = $\Delta P / \Delta T$



Red contour :
Clausius-Claperyron relation 7.5 %/C



Precipitation efficiency

East Asia average
(100-150E, 20-50N)

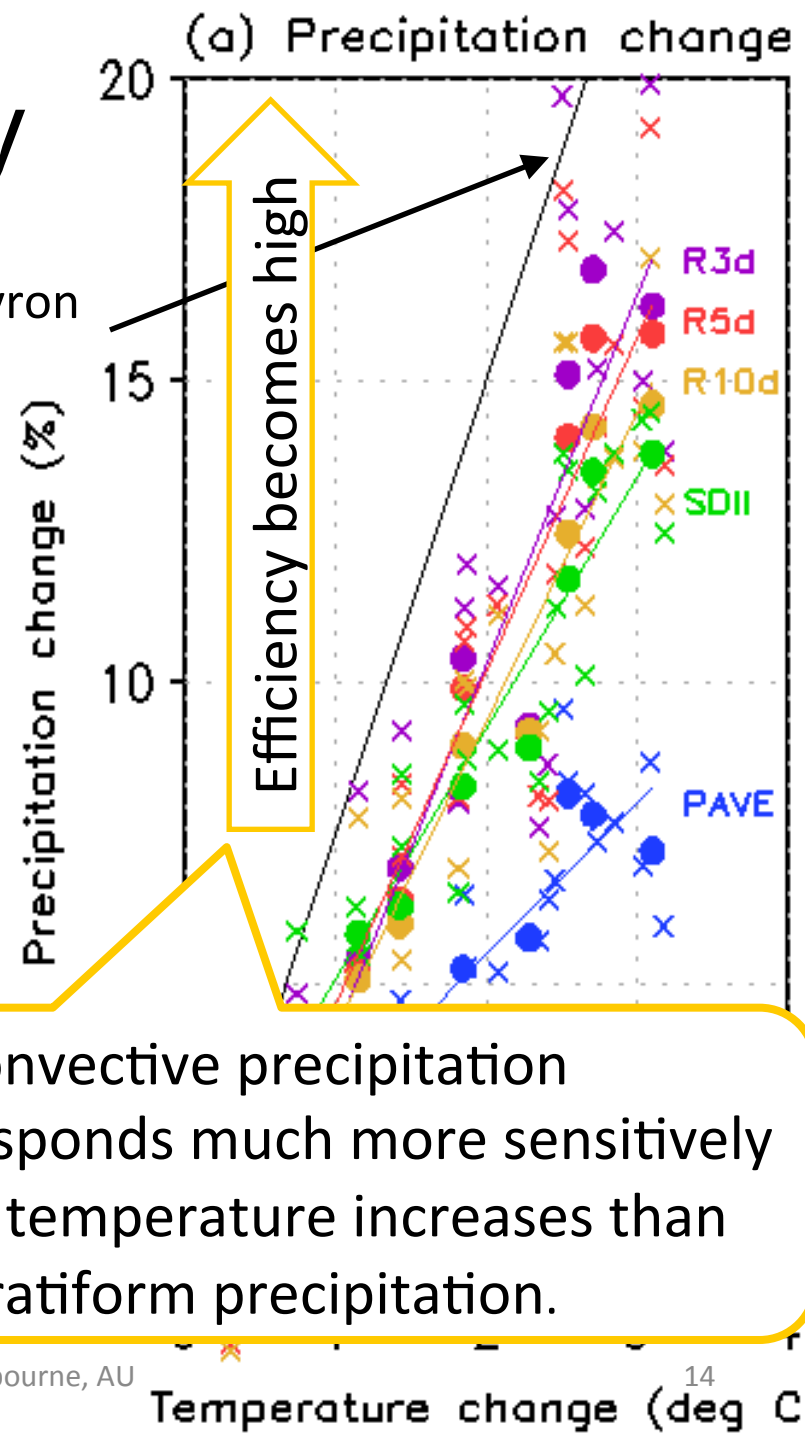
Clausius-Claperyron
relation 7.5 %/C

Decadal average
from 2010-2019 up to 2090-2099

X : Individual runs

● Ensemble average

Gradient of line :
Precipitation efficiency =
Precip change / SAT change



Summary for Topic 1

1. MRI-AGCM3.2H captures the precipitation indices well in the present-day climate.
2. All the precipitation indices will increase in the 21st century.
3. Conversion of precipitation from water vapor is more efficient for short-term precipitation than long-term precipitation.



Background

for decreasing trend in tropical cyclone frequency

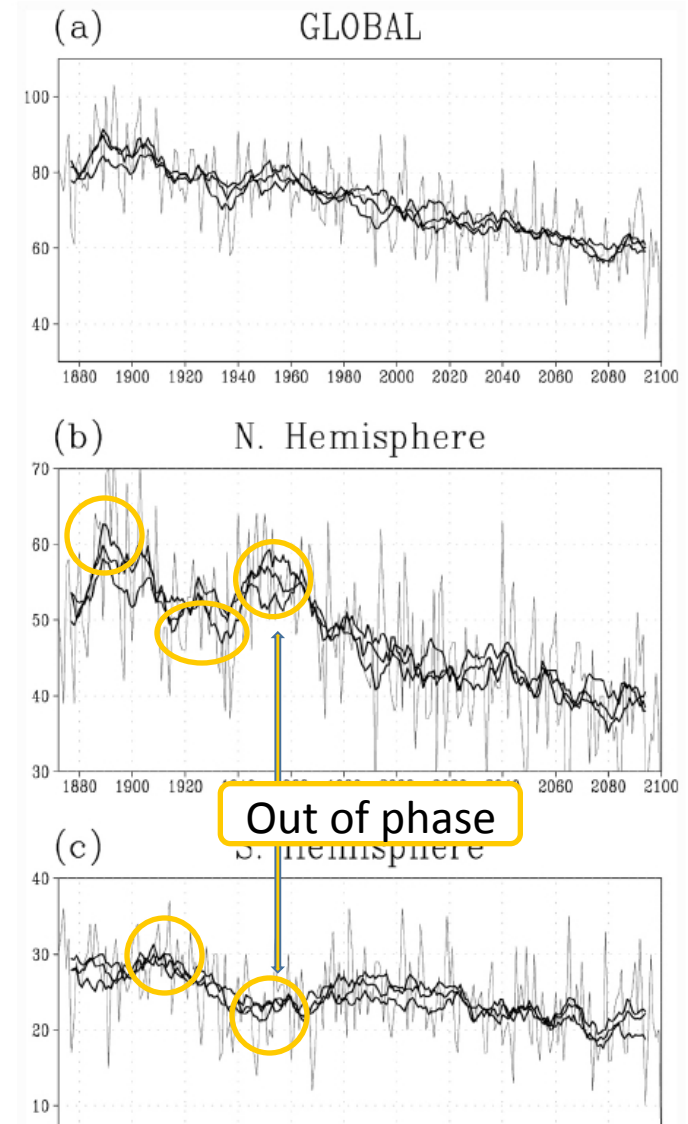
- Observed changes in tropical cyclone (TC) frequency in the 20th century are controversial (e.g. Knutson et al. 2010)
- Recent models consistently project a reduction of global TC frequency in the future due to global warming. (e.g. Sugi et al. 2002; Knutson et al. 2010)

Then, how do the models simulate the past long-term variation of TC frequency?



Long-term variation of TC Frequency

- Clear decreasing trend in both the 20th and 21st century
- Multidecadal variation
 - NH: maxima: 1890 and 1950
minimum: 1920-1940
 - SH: maximum: 1910
minimum: 1950
- Three ensemble member show a considerable difference on a decadal-scale variations



TC frequency is not fully controlled by the SST.

Decreasing trend and decadal variability

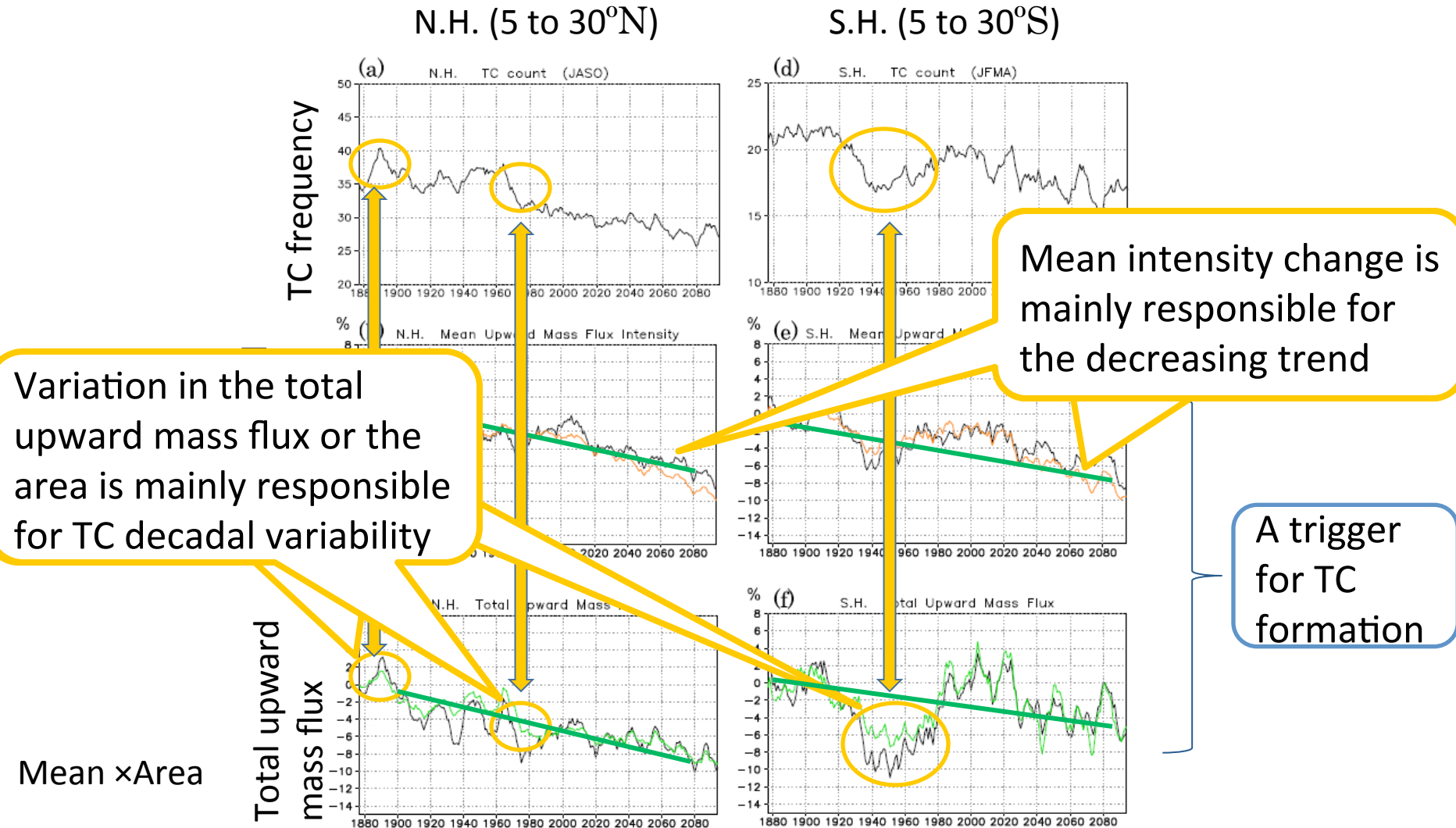
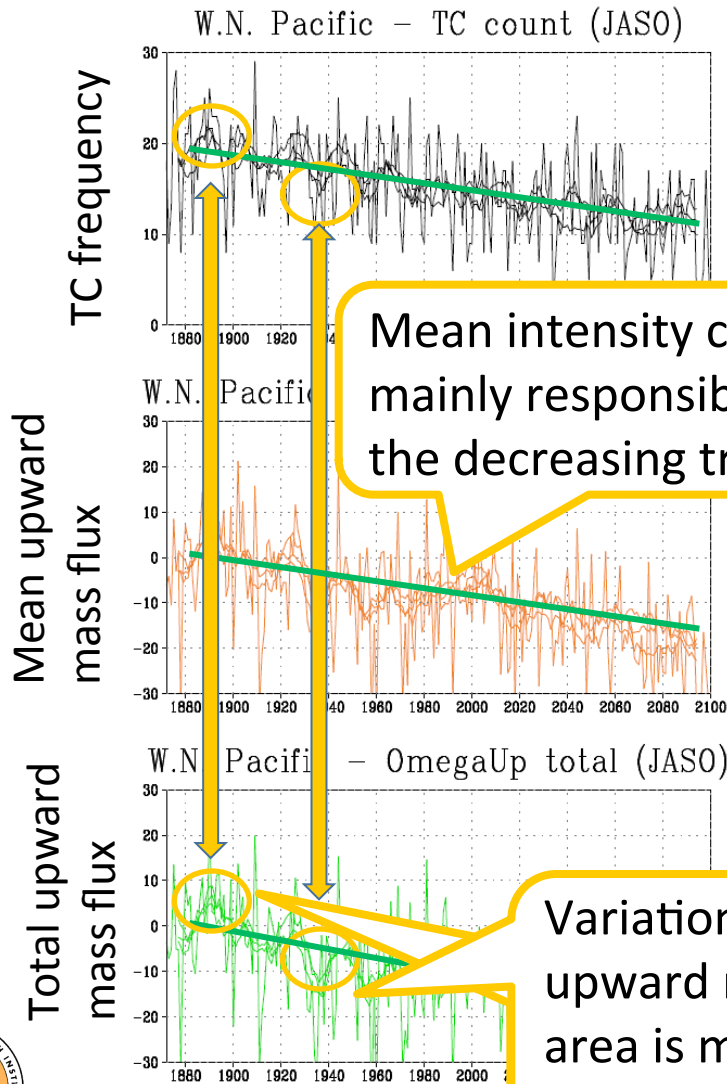


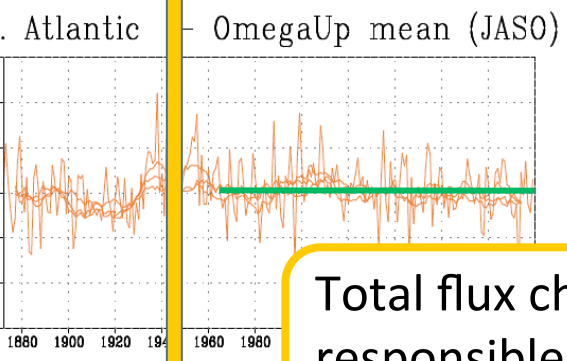
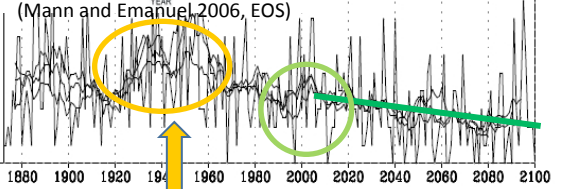
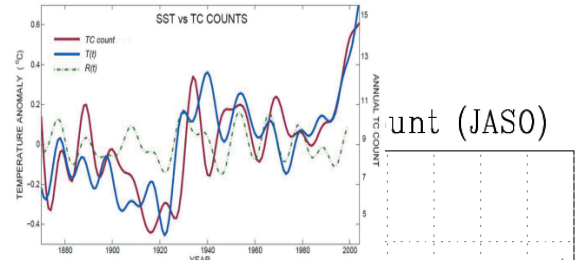
Figure 2. 11-year running average of ensemble mean of (a) TC count for NH TC genesis region (ocean between 5°N and 30°N) and for the active NH TC season (July–October), (b) mean upward mass flux intensity and (c) total upward mass flux. Orange curve in Figure 2b and green curve in Figure 2c indicates upward mass flux calculated by equation (1). (d–f) Same as in Figures 2a–2c but for SH TC genesis region (ocean between 5°S and 30°S) and active SH TC season (January–April).

Each Region in the N. H.

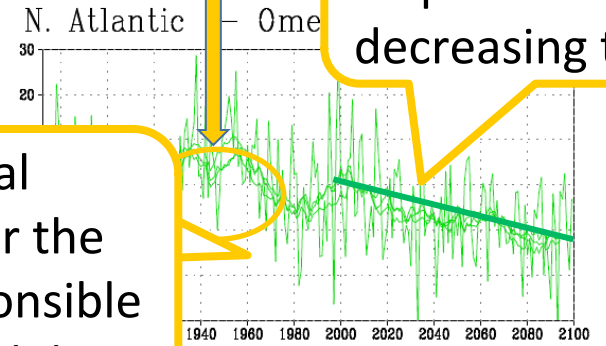


Mean intensity change is mainly responsible for the decreasing trend

Variation in the total upward mass flux or the area is mainly responsible for TC decadal variability



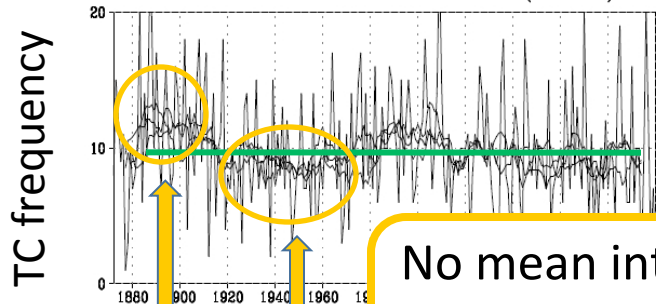
Total flux change is responsible for the decreasing trend



Each Region in the S. H.

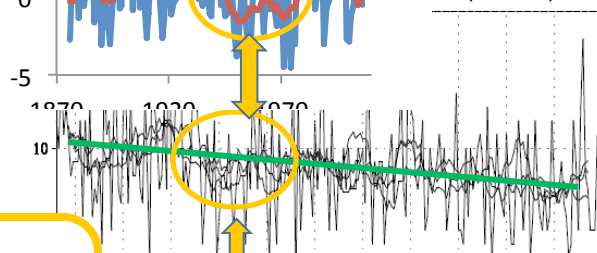
IPO

S. Indian - TC count (JFMA)



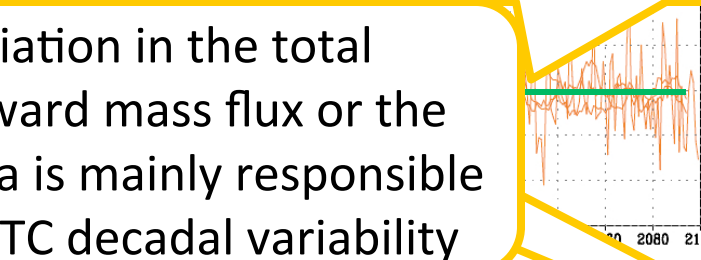
No mean intensity change is mainly responsible for no trend.

t (JFMA)



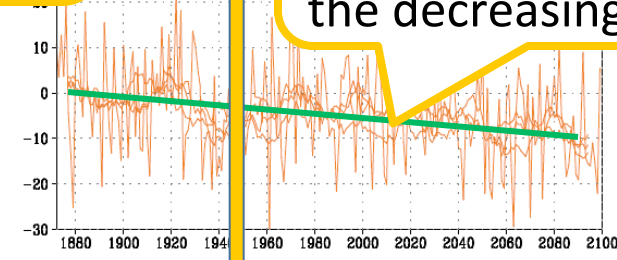
Mean intensity change is mainly responsible for the decreasing trend

S. Indian - OmegaUp total (JFMA)

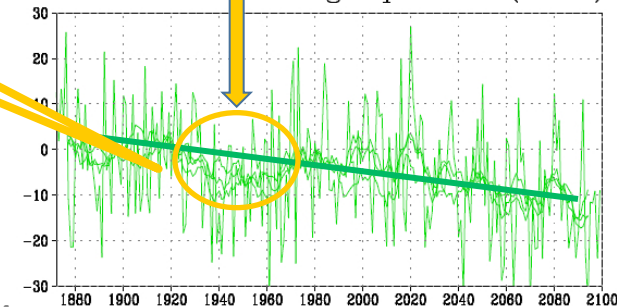


Variation in the total upward mass flux or the area is mainly responsible for TC decadal variability

S. Pacific - TC count (JFMA)



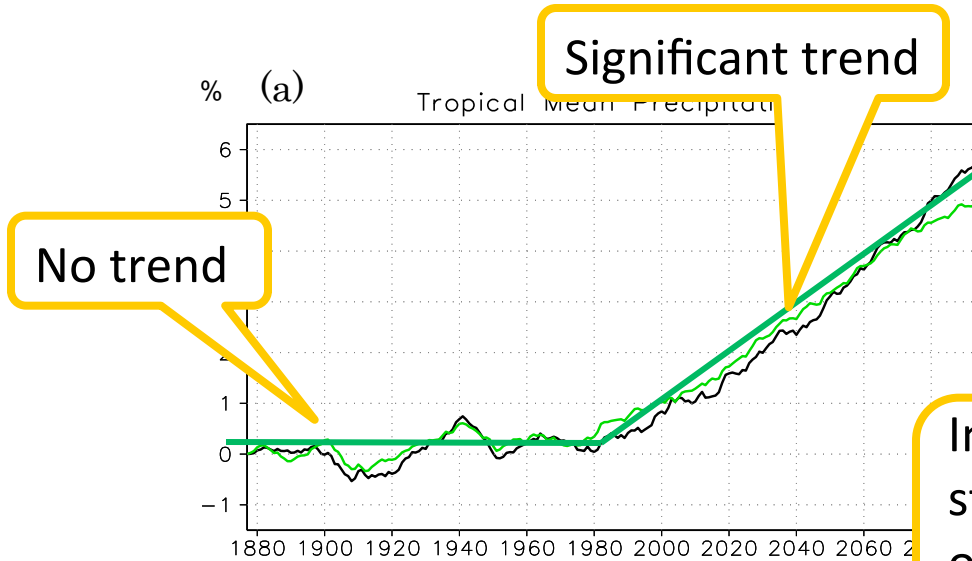
S. Pacific - OmegaUp total (JFMA)



Total upward mass flux



Long-term changes in the tropical means



Long-term changes (11-year running average of anomaly from the first thirty year mean) in the tropics mean precipitation averaged between 20°N and 20°S

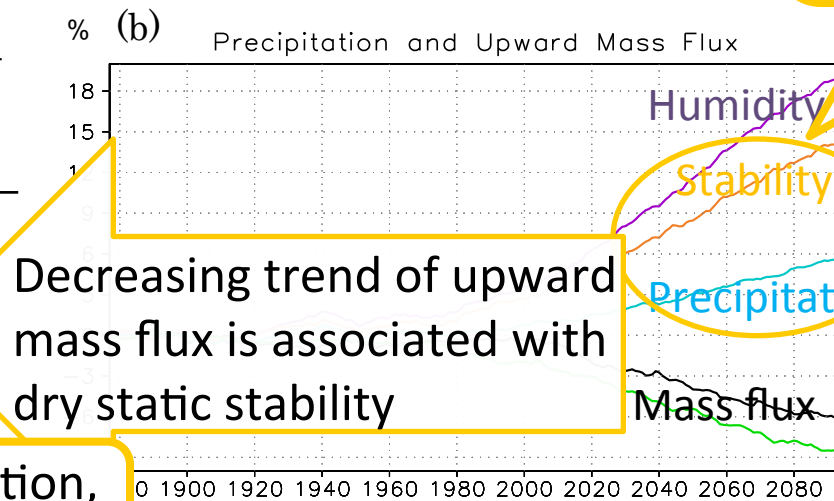
Increasing rate of the dry static stability close to that of humidity is much larger than that of precipitation

Relation in fractional ΔP , ΔS , and $\Delta \omega$

$$\frac{\Delta \omega}{\omega} \approx \frac{\Delta P}{P} - \frac{\Delta S}{S}$$

$$\frac{\Delta P}{P} < \frac{\Delta S}{S}$$

$$\frac{\Delta \omega}{\omega} < 0$$



Changes (anomaly from the first thirty year mean, unit is %) in surface specific humidity (purple line), dry static stability (orange line), precipitation (blue line), simulated upward mass flux (black line) and upward mass flux calculated by the Equation (green line).

Trigger of TC formation, $\Delta \omega$, is controlled by ΔS

Summary for TC

1. The decreasing trend and MDV in the long term variation of TC frequency correspond well to a similar decreasing trend and MDV of upward mass flux.
2. Different basins have unique features of the relationship between TC frequency and upward mass flux.
3. The upward mass flux decreases primarily because the rate of increase of dry static stability is much larger than the rate of increase of precipitation.

Key to change in TC frequency